NBSIR 86-3046

10-60 GHz G/T MEASUREMENTS USING THE SUN AS A SOURCE—A PRELIMINARY STUDY

William C. Daywitt

National Bureau of Standards
U.S. Department of Commerce
Boulder, Colorado 80303

April 1986

NBSIR 86-3046

10-60 GHz G/T MEASUREMENTS USING THE SUN AS A SOURCE— A PRELIMINARY STUDY

William C. Daywitt

Electromagnetic Fields Division
Center for Electronics and Electrical Engineering
National Engineering Laboratory
National Bureau of Standards
Boulder, Colorado 80303

April 1986

U.S. DEPARTMENT OF COMMERCE, Malcolm Baldrige, Secretary

NATIONAL BUREAU OF STANDARDS, Ernest Ambler, Director

CONTENTS

10-60 GHz G/T Measurements Using the Sun as a Source--A Preliminary Study

William C. Daywitt
National Bureau of Standards
Electromagnetic Fields Division
Boulder Colorado 80303

Preliminary studies show that it may be possible 1) to determine the solar flux density incident on the earth's atmosphere using a simple algorithm with an uncertainty less than 8 percent; 2) to overcome a deteriorating accuracy in atmospheric loss calculations by using a "tipping curve" measurement, and 3) to reduce star-shape correction factor uncertainty by using an equivalent solar diameter.

Key words: atmospheric loss, G/T, millimeter wave, solar radio flux, star-shape correction factor, tipping curve.

1. Introduction

This report contains results from investigations using the sun as a calibrated noise source in earth terminal (G/T) measurements for the frequency range from 10 to 60 GHz. It is a continuation of some earlier studies [1] for the microwave region and includes 1) an estimate of the solar flux density; 2) an estimate of, and suggestions for more accurately measuring the effects of atmospheric attenuation on the measurements, and 3) an upgraded calculation of the solar rf diameter to be used in more accurate star shape correction factor estimates.

The antenna system G/T (system gain to system noise temperature ratio) can be expressed as

$$\frac{G}{T} = \frac{8\pi k(Y - 1)}{\lambda^2 S k_1 k_2} \tag{1}$$

where k is Boltzmann's constant, Y is the ratio of the power measured with the sun in the antenna mainbeam to power measured with the antenna pointed at the cold sky, λ is the measurement wavelength, S is the solar flux density incident on the earth's atmosphere, and k_1 and k_2 are the atmospheric transmission and star shape correction factors, respectively [2].

The atmospheric transmission factor accounts for the reduction in the received flux and is due to three atmospheric phenomena [3], gaseous attenuation, refractive spreading of the incident wavefront, and incoherent tropospheric scattering. It does not include attenuation and scattering from clouds, rain, fog, hail, or snow since the precision measurements envisioned here are assumed to be performed in clear, stable weather. If τ_0 is the total zenith attenuation in nepers due to the gaseous component, then

$$k_1 = e^{-\tau_0/\sin\theta} \tag{2}$$

where θ (>5 degrees) is the elevation angle to the source relative to the antenna location on the earth's surface. Details of a simplified calculation for the gaseous component are described elsewhere [4]. Attenuation due to refractive spreading and tropospheric scatter were estimated previously [1], and will be ignored in this report since their effects are small (less than 0.1 dB) relative to attenuation from the gaseous absorption of the atmosphere.

The star shape correction factor accounts for variation of the solar brightness distribution across the antenna beam pattern, and vanishes as the ratio of the angular source diameter to the antenna half-power beamwidth vanishes. In terms of a brightness distribution B and a normalized power pattern P_n,

$$k_1 = \frac{\int B(\Omega)P_n(\Omega)\, d\Omega}{\int B(\Omega)\, d\Omega} \tag{3}$$

where Ω represents the polar angles of the antenna pattern, and $d\Omega$ is the differential solid angle. The integral in the denominator is equivalent to the flux density S.

The measurement technique [12] leading to eq (1) is suitable for personnel with less expertise than that required to determine the G/T ratio by separate G and T measurements. This radio star technique for measuring G/T assumes the availability of predetermined solar flux data and a relatively simple method for determining atmospheric attenuation. It is in the spirit of this personnel constraint that the study reported here was performed. Thus, section 2 describes a simple method for obtaining the solar flux density incident on the earth's atmosphere. This technique is still in the proposal stage and needs further experimental verification. An apparently viable,

simple method for obtaining atmospheric loss is discussed in section 3. In section 4 an equivalent disk model for more accurate evaluation of the star shape correction factor, k_2, is discussed.

2. An Estimate of the Solar Flux Density from 10 to 60 GHz

Solar radio emission is the result of three superimposed sources of radiation [5], the quiet, slow, and burst components. The quiet sun emission comes from unlocalized, thermal sources in the solar atmosphere (chromosphere and corona), and is constant over periods of months to years. The slow component is also thermally generated and originates in local sources in the vicinity of sunspots and chromospheric plaques. These partially polarized sources have periods of days, weeks, or months. The burst components are the results of thermal, synchrotron, and plasma radiation from transient sources such as flares, and are partially polarized. Their recurrence frequency and period are small for the quiescent portion of the solar cycle, increasing to two or more per a 10-hour viewing day during the active portion, and suggest the possibility of making G/T measurements without encountering a burst during the process.

Figure 1 depicts the average solar flux density spectrum incident on the earth's atmosphere [6] with an insert [7] indicating the duration of the burst spectrum from 10 MHz to 30 GHz. The quiet component of the solar emission dominates above 5 GHz, at which frequency most of the burst components have disappeared and the slow component is falling off. The insert shows that the duration of the remaining burst continuum is short. Thus, the solar emission above 5 GHz is relatively stable from day to day as long as the type IV bursts are avoided. Superimposed on the graph of figure 1 are three sets of hash-marks representing monthly averages of AFGL (Air Force Geophysical Laboratory) flux density measurements [8] from January 1979 to May 1982. As expected, the measurement values approach the quiet sun values between the "sunspot (s.s.) max" and the "s.s. min" curves as the frequency increases. Thus, it appears that the average of the quiet sun curves might be used to determine the incident flux density. Following is an approximate equation giving this average that was derived by a quadratic least-square fitting of the data in table 1 from reference [6]

$$\log S = 1.20 + 1.10 (\log f) + 0.179 (\log f)^2. \qquad (4)$$

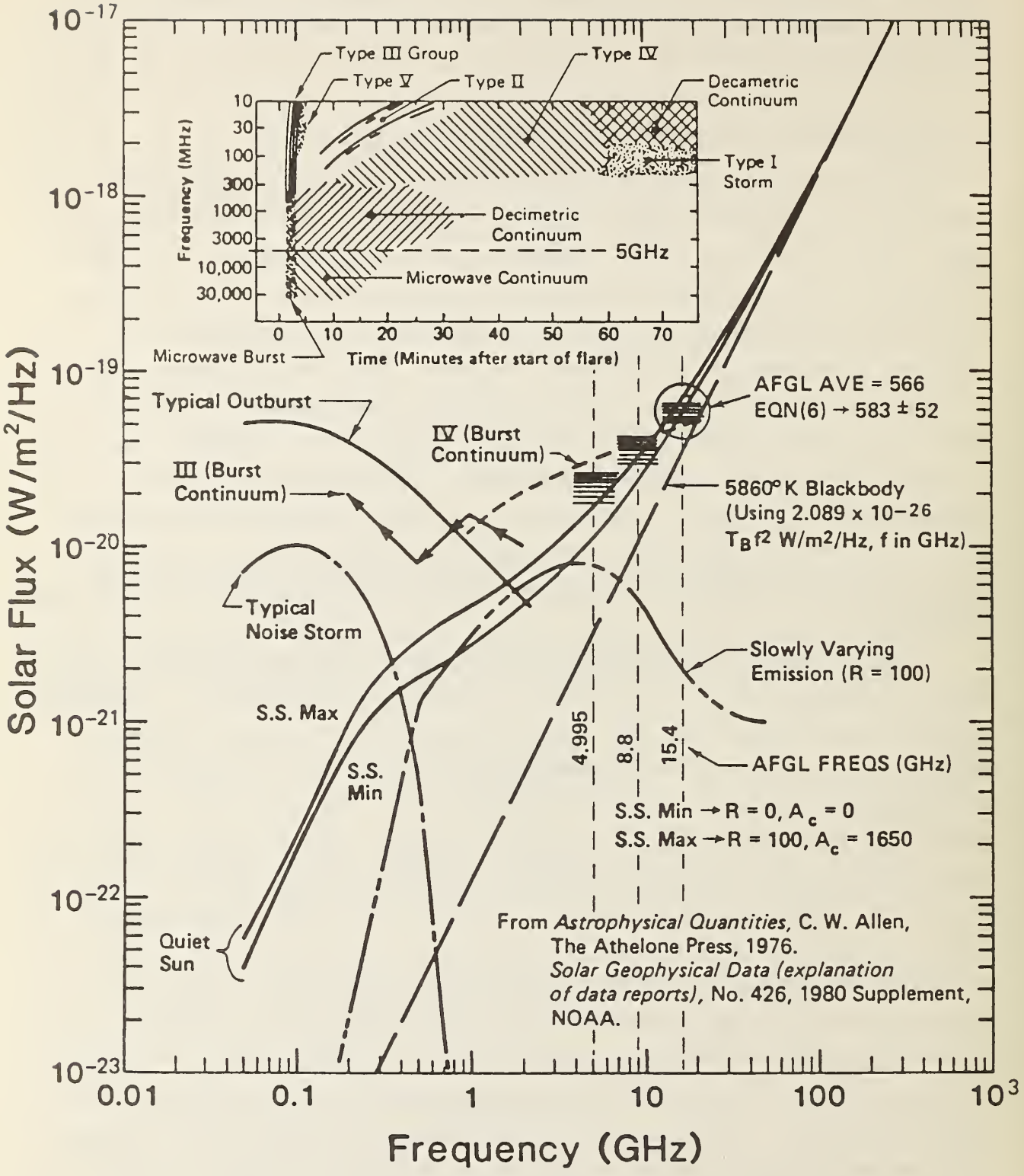

Figure 1. Solar radio spectrum.

Table 1. Logarithm to the base ten of the average flux density $S(W/m^2/Hz)$ vs frequency for the quiet sun radiation. (From Allen [6].)

QUIET SUN RADIATION	
FREQUENCY (GHz)	Log S
10	2.48
20	2.93
50	3.57
100	4.125
200	4.69
500	5.47

The error in using eq (4) is tentatively estimated to be 8 percent [1], but is in need of further verification and/or upgrading. In fact, further investigation may show that periodic measurements at least at one frequency between 10 and 60 GHz are necessary to obtain sufficiently accurate coefficients for eq (4).

3. Atmospheric Loss

An estimate [4] of the zenith attenuation through the atmosphere as a function of frequency is given by the solid curve in figure 2 for a water vapor density of 7.75 gm/m^3. The dashed curves and the right-hand scale show the corresponding error in k_1 (approximately $95(1-k_1)$) for two elevation angles (30° and 90°), and indicate that above 10 GHz another method must be found for determining the loss if a tolerable G/T measurement accuracy is to be maintained. A number of versions [9,10,11] of the "tipping curve" technique (to be described) have been used to measure the loss and appear to give good accuracy. For example, Ulich [10] reports an error ($20(1-k_1)$) nearly five times less than that obtainable from the preceeding calculation [4]. Therefore, since the present earth terminal measurement system (ETMS) [12] accumulates tipping-curve data automatically during a G/T measurement,

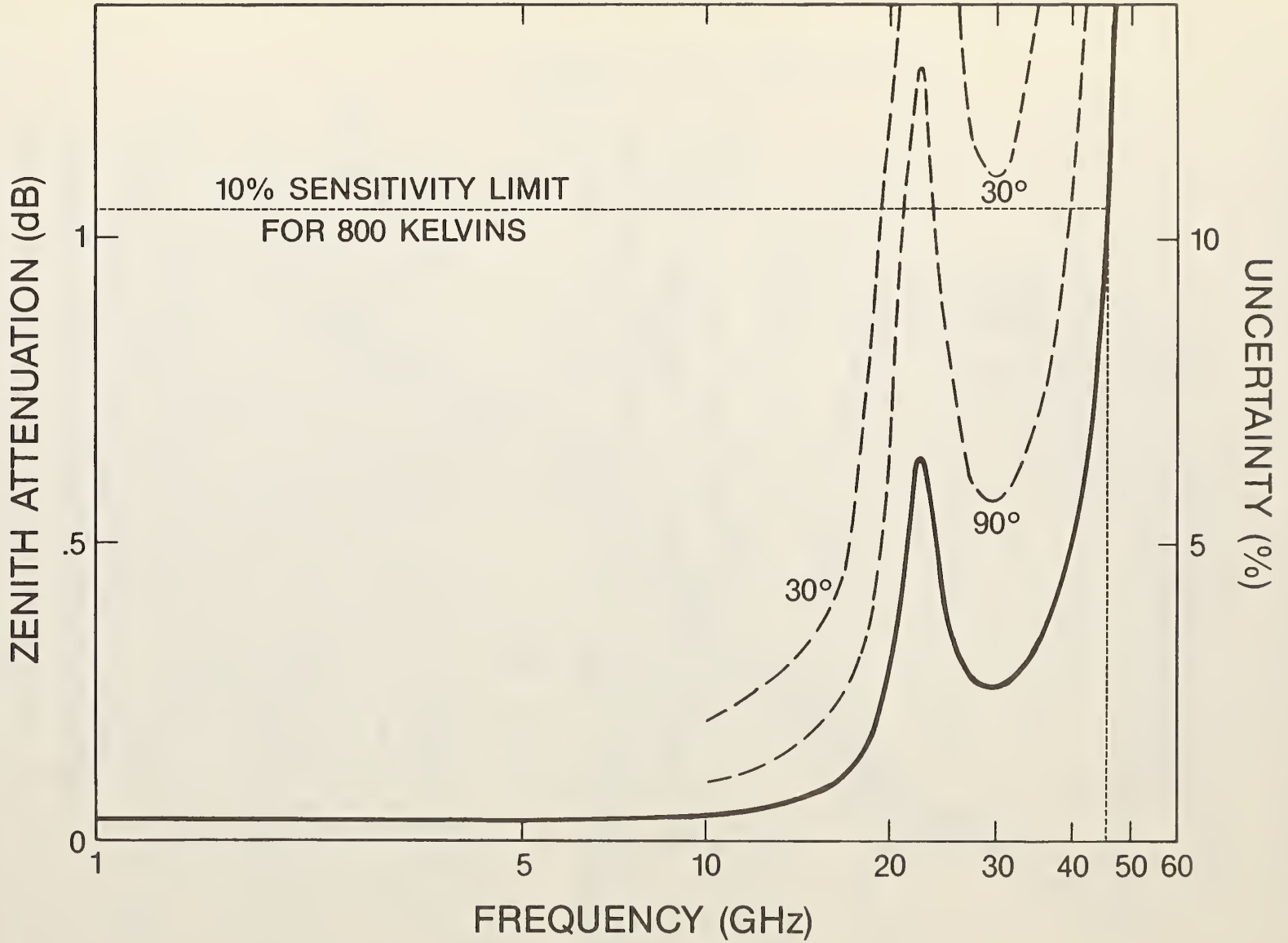

Figure 2. Zenith attenuation as a function of frequency caused by atmospheric absorption. Calculations are based on the 1962 standard atmosphere starting from a surface temperature, pressure, and water vapor density of 300 K, 1013.24 mb, and 7.75 gm/m^3, respectively. The dashed curves represent the corresponding uncertainty in the calculations of k_1 at zenith and at 30° elevation angle. The dotted lines are explained in section 3 of the text.

this data can be used to obtain a more accurate loss estimate. What follows is the description of a slightly different version of the tipping-curve method using "noise add" which is appropriate to the type of data collected by the ETMS.

Figure 3 shows a measurement system consisting of an antenna, a cross-guide coupler, a receiver, and a power meter. A noise source that can be rapidly turned on and off is attached to one arm of the coupler. The slanted, cross-hatched area at the left of the diagram represents the atmosphere extending down to the antenna at the earth's surface, and that is viewed at an angle θ (the elevation angle) relative to the horizontal. T_c at the far left (above the atmosphere) represents the incident isotropic, cosmic background temperature [13]. T_m is an average atmospheric temperature [9] that allows the sky brightness temperature T_x to be accurately calculated by the formula

$$T_x = T_c\, e^{-\tau_x} + T_m(1 - e^{-\tau_x}) \tag{5}$$

where τ_x is the slant height loss (neper attenuation) through the atmosphere and is related to the elevation angle ($x = \csc\theta$) and the zenith loss τ_0 by the equation

$$\tau_x = x\, \tau_0. \tag{6}$$

The curved, dashed line around the antenna aperture representing the incident sky flux is a reminder that the flux is considered to be constant over the antenna beam. In effect, the antenna is assumed to be in an isothermal cavity of brightness temperature T_x. α represents the noise efficiency [14] of the antenna-coupler combination. The receiver noise, including the noise from the ohmic losses in the antenna and coupler, is represented by T_e. The attenuated noise temperature due to the sky, and appearing at the receiver input is given by αT_x, while the noise from the noise source (when the source is turned on) appearing at this same point is represented by T_n. The corresponding down-converted powers at the power meter are p_e, p_x, and p_n, respectively.

In performing a measurement at a particular x, two powers are measured; one with $(P_x + P_e + P_n)$ and one without $(P_x + P_e)$ the noise source in figure 3 turned on; and the following Y-factor ratio is calculated;

$$y_x = \frac{p_x + p_e}{p_n} \tag{7}$$

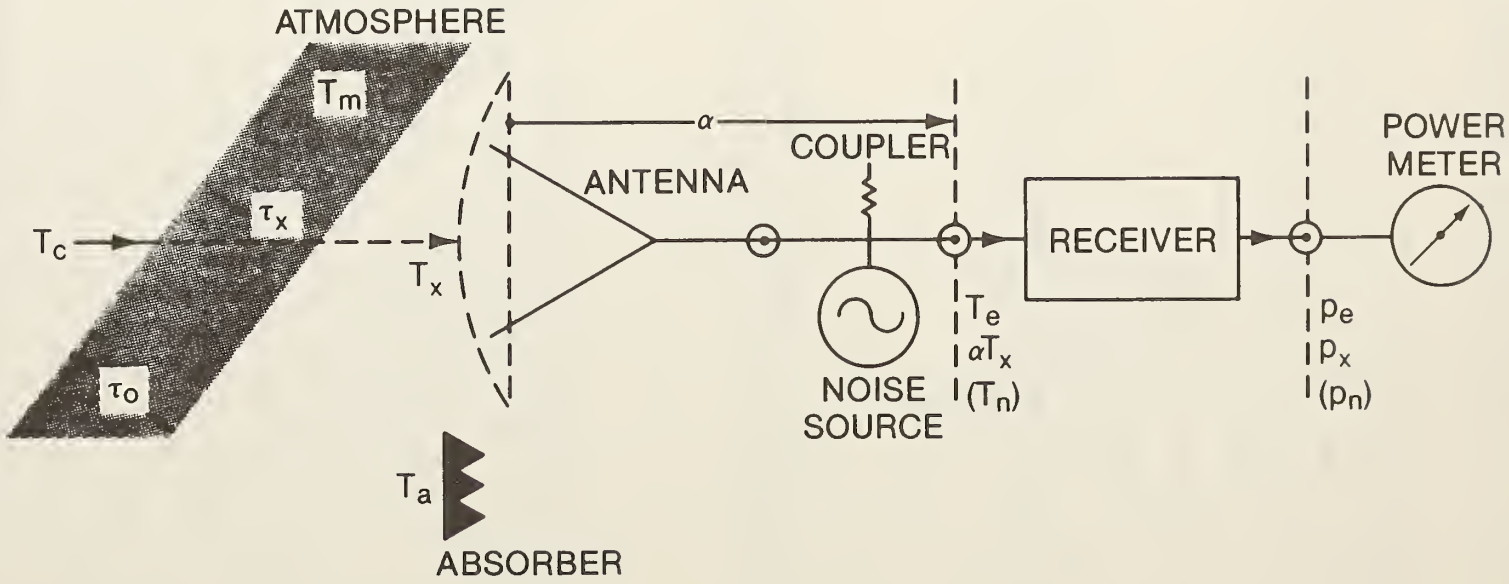

Figure 3. A simple model for the atmosphere and a satellite earth terminal receiving system.

from which the radiometer calibration equation (eq (8)) is obtained (errors due to receiver gain variations are removed from the measurement by taking the ratio in eq (7) [15,16]):

$$T_x = a\, y_x - b \tag{8}$$

where a and b are functions of the antenna system parameters and the noise add signal T_n. In terms of noise temperatures, "a" is equivalent to the noise add signal referred to the antenna aperture, T_n/α, and "b" is equivalent to the receiver noise referred to the aperture, T_e/α.

τ_0 can be determined in one of two ways: the two constants, a and b, in eq (8) can be determined from two known values of T_x; or from one value of T_x and the use of an absorber of known temperature (T_a in fig. 3) in the antenna aperture. Since τ_0 is initially unknown, the second or tipping curve scheme is used in a manner [11] similar to the following simplified description. The antenna is pointed to zenith (some other elevation angle could be used) and the Y-factor, y_1, is measured, corresponding to which a preliminary value of zenith loss is assumed and a preliminary brightness temperature $\hat{T}_x$ calculated. An absorber is inserted into the antenna aperture and the Y-factor y_a measured. These values are then used to obtain an initial estimate of the constants in eq (8). A number of other Y-factors are measured at various elevation angles, for which their corresponding brightness temperatures are estimated from eq (8). Using these estimates the following equation is plotted as a function of x (see eq (5)):

$$\hat{\tau}_x = \ln\left(\frac{T_m - T_c}{T_m - \hat{T}_x}\right) \tag{9}$$

where the circumflex accents above τ_x and T_x indicate that these values are preliminary estimates. A straight line is fit through the resulting points, and extended to the ordinate. Equations (5) and (6) imply that the resulting intercept should be at the origin. If this is not the case, the preceding steps are repeated until the extended line passes through the origin, at which point the assumed value of zenith loss is the correct one, and the atmospheric loss has been determined.

The usefulness of the above technique is limited by the system noise which masks changes in the antenna noise temperature caused by the tipping-

curve procedure. Assuming a minimum useful change of 0.1 * T_e in the antenna temperature between x = 1 and x = 3, the tipping-curve method appears to work up to a zenith attenuation of about 1.04 dB for a T_e of 800 K. Thus, the dotted lines in figure 2 indicate that a direct application of the tipping-curve technique at the frequency of interest should be useful up to some frequency between 40 GHz and 50 GHz. Above this frequency a dual-channel approach [11] in conjunction with calculations might be used to determine the atmospheric loss.

4. Star-Shape Correction Factor

For antenna half-power beamwidths (HPBW) greater than about five angular source diameters, examination of eq (10) below shows that the ratio in eq (3) can be replaced by unity with an error less than 1 percent. However, to use the celestial source method of measuring G/T accurately when the HPBW is less than five source diameters requires an estimate of the variation of the source brightness distribution across the antenna mainbeam, as indicated in eq (3). For sources with stable and predictable distributions and antennas with Gaussian mainbeams, this can be accomplished by replacing the ratio in eq (3) by a simple formula [17] depending only on the ratio of HPBW to source diameter. Furthermore, if the source diameter is properly chosen, the formula will provide an accurate estimate of the correction factor for any HPBW/diameter ratio above unity [18,19]. As will be seen there is reason to expect that this technique will also work for the sun, even though the solar brightness temperature is continuously changing.

For a Gaussian mainbeam and a source resembling a circular disk, eq (3) leads to (note that x is redefined)

$$k_2 = \frac{1 - e^{-x^2}}{x^2} \tag{10}$$

where

$$x^2 \equiv \left(\frac{d_e}{\theta_H}\right)^2 \ln 2. \tag{11}$$

d_e is an equivalent angular disk diameter for the source, and θ_H is the antenna HPBW. The diameter is chosen to minimize the difference

$$\frac{1 - e^{-x^2}}{x^2} - \frac{\int B(\Omega)\, P_n(\Omega)\, d\Omega}{\int B(\Omega)\, d\Omega} \tag{12}$$

for θ_H/d greater than unity, where d is the apparent or optical solar angular diameter. The same expressions (eqs (10) and (11)) hold for an elliptical disk with d_e^2 replaced by the product of the major and minor source diameters. No significant reduction in the difference in eq (11) is achieved with this latter model, however, even though the solar brightness distribution shows a decided ellipticity [5].

Figure 1 shows that, except for the burst components which are assumed to be missing during the G/T measurement, the quiet sun emission plays an increasingly dominant role in the total emission above 5 GHz where the slow component begins to fall off. Furthermore, observations of the solar brightness distribution in the decimeter, centimeter, and millimeter wave frequency regions reveal that, although the effective brightness temperature varies with the solar cycle, the distributions remain relatively constant [5]. It is this constant part of the brightness distribution that will presumably be amenable to the technique of the previous paragraph, with fluctuations in the result coming from the more variable slow emission component. The degree of success will depend upon how minor these fluctuations turn out to be, but hopefully at least some accuracy in k_2 will be gained below five source diameters. This question can only be decided after a number of actual distributions at various frequencies and at various times during the solar cycle have been convoluted with the antenna beam pattern. To date this has not been done.

The equivalent disk diameter described here was calculated from an approximation (fig. 4, dashed curves) to the solar atmosphere tabulated in Allen [6] (fig. 4, solid curves) using the dynamical equations described by Smerd [20] to obtain the solar brightness temperature. The resulting disk diameter (normalized by the apparent solar diameter) is shown in figure 5 for the frequency range from 1 to 100 GHz. As a matter of interest, the disk diameter obtained using Smerd's earlier atmosphere is also shown in the figure (dashed curve).

The uncertainty in k_2 due to using the apparent diameter ($d_e = d$) to calculate the star shape correction factor via eq (10) is shown in figure 6 as a function of the ratio of antenna half-power beamwidth to apparent diameter. After minimizing this uncertainty per the discussion surrounding eq (12) and using the resulting equivalent diameter ($d_e = 1.0342d$), the uncertainty in using eq (10) to estimate the integral in eq (12) is negligible.

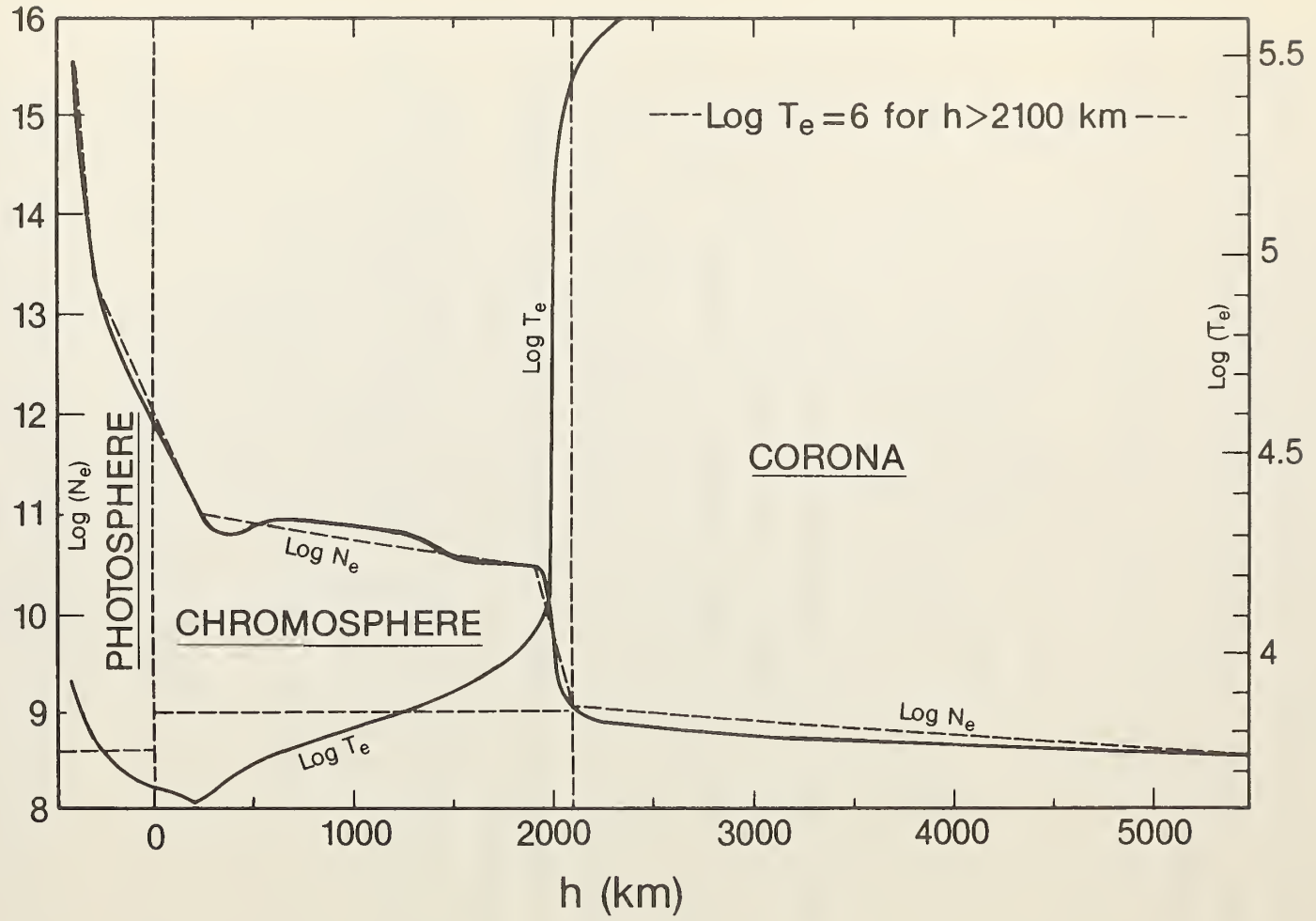

Figure 4. Approximations (dashed curves) to the electron temperature T_e (kelvins) and density $N_e(cm^{-3})$ of a model [6] solar atmosphere (solid curve).

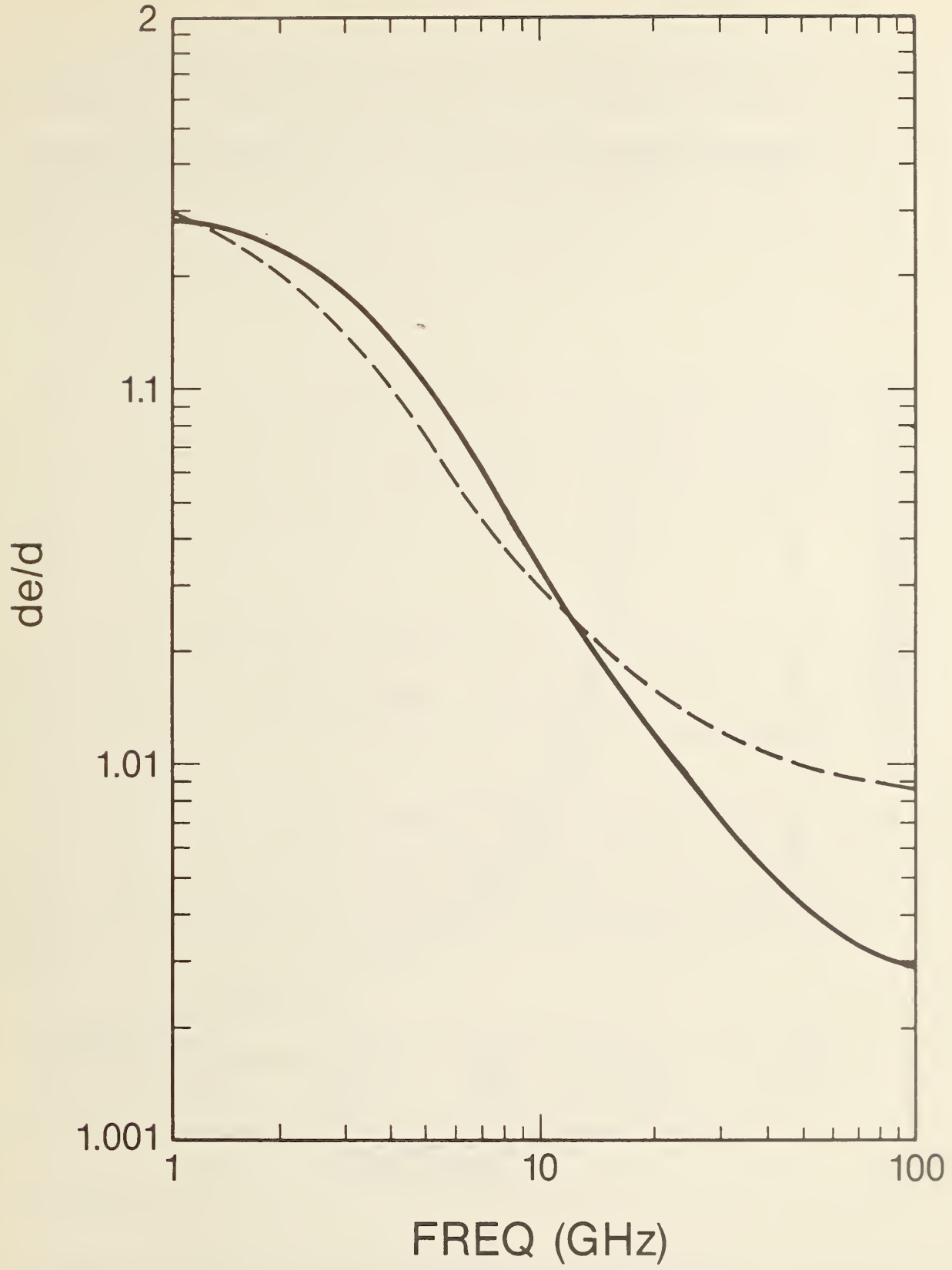

Figure 5. Equivalent disk diameter d_e in units of the apparent solar diameter d as a function of frequency using 1) data from Allen [6], solid curve; and 2) data from Smerd [20], dashed curve.

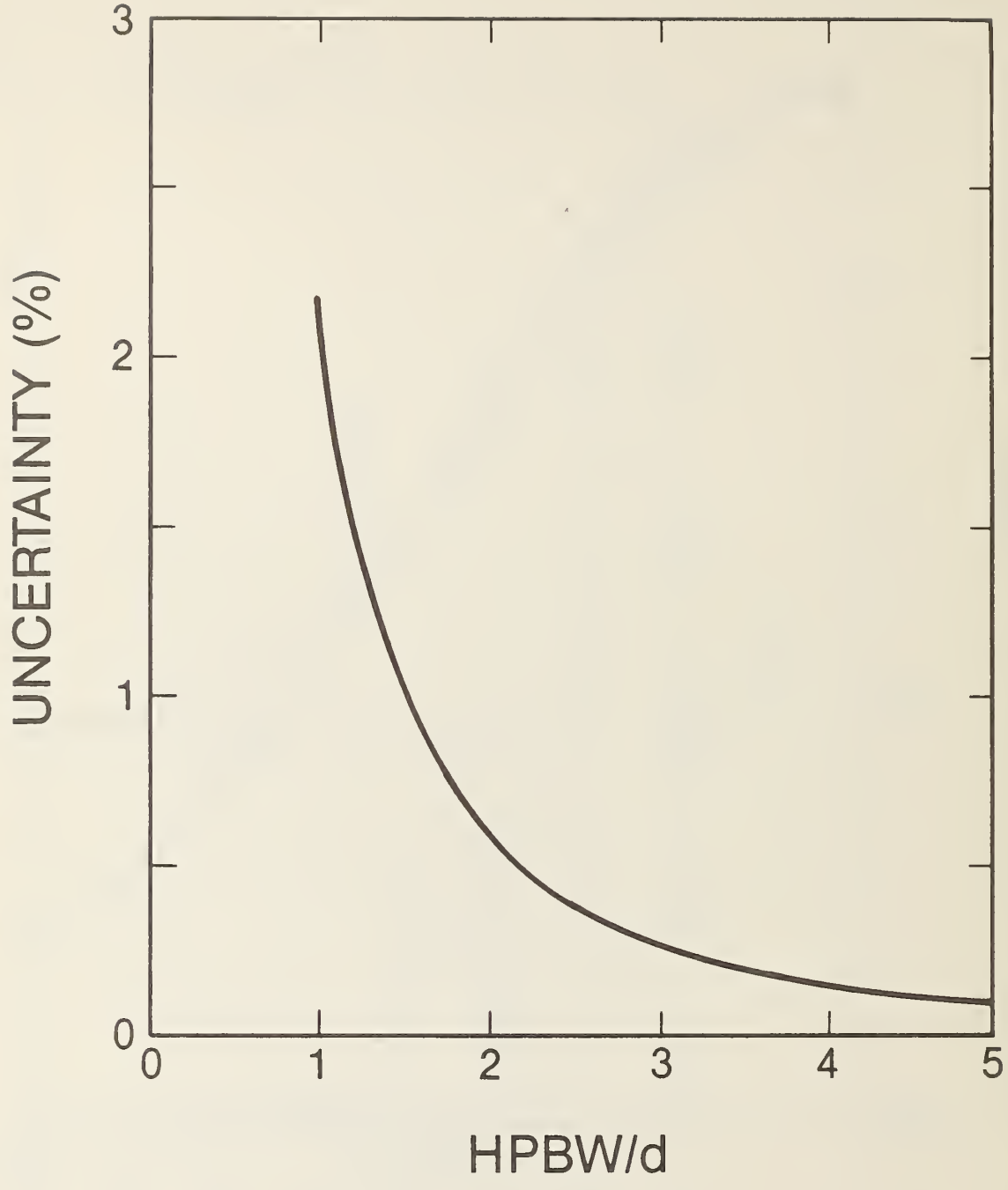

Figure 6. Uncertainty in the star shape correction factor vs HPBW (in units of the apparent solar diameter) due to using the apparent solar diameter in eq (10). When an equivalent disk diameter equal to 1.0342d is used, the uncertainty is negligible.

An accurate description of the solar brightness temperature at cm- and mm-wavelengths requires accounting for the chromospheric fine structure [21]. The resulting two-component solar atmosphere [22] includes radiation from both the chromospheric spicular and the interspicular regions and their variation with height. These details have not been included in the preceeding calculations of the equivalent diameter.

5. Conclusions

Equation (4) is an algorithm for calculating the solar flux density incident on the earth's atmosphere, with an estimated uncertainty of 8 percent. Experiments need to be performed to see if this uncertainty can be reduced and/or to improve the coefficients in eq (4). Furthermore, it may be necessary to periodically measure the solar flux density and update the coefficients.

It may be possible to overcome the deteriorating accuracy in earlier atmospheric loss calculations [4] by incorporating a tipping curve measurement into the ETMS G/T measurement scheme. If this improvement is not possible, on-site measurement of the loss by more sophisticated instrumentation [11] will be required.

Simple and accurate calculations of the star shape correction factor using eq (10) may be possible, but need to be verified by experimental data. Although straightforward, the effects of chromospheric fine structure still need to be incorporated into the calculation of the equivalent solar disk diameter.

6. Acknowledgement

The author wishes to thank the Air Force Satellite Control Facility at the Sunnyvale Air Force Station for support of these studies.

7. References

[1] Daywitt, W. C. A preliminary investigation into using the sun as a source for G/T measurements. Nat. Bur. Stand. (U.S.) Int. Rpt. 84-3015; 1984 August.

[2] Daywitt, W. C. Error equations used in the NBS precision G/T measurement system. Nat. Bur. Stand. (U.S.) Int. Rpt. 76-842; 1976 September.

[3] Yokoi, H.; Yamada, M.; Satok, T. Atmospheric attenuation and scintillation of microwaves from outer space. Publ. Astr. Soc. Japan. 22(4): 511-524; 1970.

Yamada, M.; Yokoi, H. Measurements of earth-space propagation characteristics at 15.5 GHz and 31.6 GHz using celestial radio sources. J. of the Inst. of Electronics and Communication Engineers of Japan. 57-B(2); 1974 February.

[4] Daywitt, W. C. Atmospheric propagation equations used in the NBS earth terminal measurement system. Nat. Bur. Stand. (U.S.) Int. Rpt. 78-883; 1978 April.

[5] Kundu, M. R. Solar radio astronomy. New York: Interscience Publishers; 1965.

[6] Allen, C. W. Astrophysical quantities. London, England: The Athlene Press/University of London; 1976.

[7] Mangis, S. J. Introduction to solar-terrestial phenomena and the space environment services center. NOAA Tech. Rpt. ERL 315-SEL 32; 1975 January.

[8] Coffey, H. E., ed. Solar-geophysical data: prompt reports. No. 470, Part 1; 1983 November.

[9] Falcone, V. J., Jr.; Wulfsberg, K. N.; Gitelson, S. Atmospheric emission and absorption at millimeter wavelengths. Rad. Sci. 6(3): 347-355; 1971 March.

[10] Ulich, B.; Davis, J. H.; Rhodes, P. J.; Holis, J. M. Absolute brightness temperature measurements at 3.5-mm wavelength. IEEE Trans. on Ant. and Propag. AP-28(3); 1980 May.

[11] Guirand, F. O.; Howard, J.; Hogg, D. C. A dual-channel microwave radiometer for measurement of precipitable water vapor and liquid. IEEE Trans. on Geosci. Elect. GE-17(4); 1979 October.

Hogg, D. C.; Guirand,F. D.; Westwater, E. R. Emission measurements of 31.6 GHz absorption by atmospheric water vapor. Rad. Sci. 18(6): 1295-1300; 1983 November-December.

[12] Wait, D. F. Precision measurements of antenna system noise using radio stars. IEEE Trans. on I&M. IM-32(1): 110-116; 1983 March.

[13] Penzias, A. A.; Wilson R. W. A measurement of excess antenna temperature at 4080 mc/s. Astro. J. 142: 419-421; 1965.

[14] Daywitt, W. C. Design and error analysis for the WR10 thermal noise standard. Nat. Bur. Stand. (U.S.) Tech. Note 1071; 1983 December.

[15] Ohm, E. A.; Snell, W. W. A radiometer for a space communications receiver. The Bell System Technical Journal; 1963 September.

[16] Stelzried, C. T. Total power and noise adding radiometers. From notes for high-frequency and microwave noise seminar. Nat. Bur. Stand. (U.S.); 1970 May.

[17] Baars, J. W. M.; Mezger, P. G.; Wendker, H. The spectra of the strongest nonthermal radio sources in the centimeter-wavelength range. Astr. J. 142: 122-134; 1965.

[18] Kanda, M. Study of errors in absolute flux density measurements of Cassiopeia A. Nat. Bur. Stand. (U.S.) Int. Rpt. 75-822; 1975 October.

[19] Daywitt, W. C. An error analysis for the use of presently available lunar radio flux data in broadbeam antenna system measurements. Nat. Bur. Stand. (U.S.) TEch. Note 1073; 1984 February.

[20] Smerd, S. F. Radio-frequency radiation from the quiet sun. Aus. J. Sci. Res. A3(34): 34-59; 1950.

[21] Fürst, E. The quiet sun at cm- and mm-wavelengths. Radio Physics of the sun. M. R. Kande and T. E. Gergely, eds. STATE D. Reidel Publishing Company; 1980.

[22] Bray, R. J.; Longhead, R. E. The solar chromosphere. London: Chapman & Hall; 1974.

U S GOVERNMENT PRINTING OFFICE 1986

NBS-114A (REV. 2-8C)

U.S. DEPT. OF COMM. BIBLIOGRAPHIC DATA SHEET (See instructions)	1. PUBLICATION OR REPORT NO. NBSIR 86-3046	2. Performing Organ. Report No.	3. Publication Date April 1986

4. TITLE AND SUBTITLE

10-60 GHz G/T Measurements Using the Sun As A Source--A Preliminary Study

5. AUTHOR(S)

William C. Daywitt

6. PERFORMING ORGANIZATION (If joint or other than NBS, see instructions)

NATIONAL BUREAU OF STANDARDS
DEPARTMENT OF COMMERCE
WASHINGTON, D.C. 20234

7. Contract/Grant No.

8. Type of Report & Period Covered

NBSIR 1985-1986

9. SPONSORING ORGANIZATION NAME AND COMPLETE ADDRESS (Street, City, State, ZIP)

Department of the Air Force
HQ Air Force Satellite Control Facility (AFSC)
Sunnyvale Air Force Station, P.O. Box 3430
Sunnyvale, California 94088

10. SUPPLEMENTARY NOTES

☐ Document describes a computer program; SF-185, FIPS Software Summary, is attached.

11. ABSTRACT (A 200-word or less factual summary of most significant information. If document includes a significant bibliography or literature survey, mention it here)

Preliminary studies show that it may be possible 1) to determine the solar flux density incident on the earth's atmosphere using a simple algorithm with an uncertainty less than 8 percent; 2) to overcome a deteriorating accuracy in atmospheric loss calculations by using a "tipping curve" measurement, and 3) to reduce star-shape correction factor uncertainty by using an equivalent solar diameter.

12. KEY WORDS (Six to twelve entries; alphabetical order; capitalize only proper names; and separate key words by semicolons)

atmospheric loss; G/T; millimeter wave' solar radio flux; star-shape correction factor; tipping curve

13. AVAILABILITY

☒ Unlimited

☐ For Official Distribution. Do Not Release to NTIS

☐ Order From Superintendent of Documents, U.S. Government Printing Office, Washington, D.C. 20402.

☒ Order From National Technical Information Service (NTIS), Springfield, VA. 22161

14. NO. OF PRINTED PAGES

24

15. Price